

Conformational Stability, r_0 Structural Parameters, Ab Initio Calculations, and Vibrational Assignment for Fluorocyclopentane

James R. Durig,^{*,†} Ahmed M. El Defrawy,^{§,†} Arindam Ganguly,^{||,†} Todor K. Gounev,[†] and Gamil A. Guirgis[‡]

Department of Chemistry, University of Missouri—Kansas City, Kansas City, Missouri 64110, and Department of Chemistry and Biochemistry, College of Charleston, Charleston, South Carolina 29424

Received: March 20, 2009; Revised Manuscript Received: June 8, 2009

The infrared spectra (3200–50 cm^{-1}) of the gas and solid and the Raman spectrum (3200–30 cm^{-1}) of liquid and solid fluorocyclopentane, $c\text{-C}_5\text{H}_9\text{F}$, have been recorded. Additionally the infrared spectra (3200–400 cm^{-1}) of liquid xenon solutions have been recorded at -65 and -95 °C. In all of the physical states, only the twisted C_1 conformer was detected. Ab initio calculations utilizing various basis sets up to MP2(full)/6-311+G(2df,2pd) with and without diffuse functions have been used to predict the conformational stabilities. These calculations predict only the twisted C_1 conformer as the stable form. The two envelope (C_s symmetry) forms with axial and equatorial structures were predicted to be first order saddle points with average higher energies of 75 ± 33 and 683 ± 44 cm^{-1} , respectively, from the C_1 conformer but lower energies of 2442 and 1812 cm^{-1} , respectively, than the planar form by MP2 calculations. Similar values were obtained from the corresponding density functional theory calculations by the B3LYP method. A complete vibrational assignment is given for the twisted (C_1) conformer which is supported by normal coordinate calculations with scaled force constants from MP2(full)/6-31G(d) calculations. The adjusted r_0 structural parameters have been obtained by systematically fitting the MP2(full)/6-311+G(d,p) predicted values with the rotational constants obtained from a microwave study. The determined heavy atom r_0 distances in Å are $(C_1C_2) = 1.531(3)$, $(C_1C_3) = 1.519(3)$, $(C_2C_4) = 1.553(3)$, $(C_3C_5) = 1.533(3)$, $(C_4C_5) = 1.540(3)$, and $(C_1F_6) = 1.411(3)$ and the angles in degrees are $\angle C_3C_1C_2 = 105.5(5)$, $\angle C_1C_2C_4 = 106.2(5)$, $\angle C_1C_3C_5 = 102.9(5)$, $\angle F_6C_1C_2 = 108.9(5)$, and $\angle F_6C_1C_3 = 107.6(5)$ with a dihedral angle $\angle C_2C_4C_5C_3 = 25.3(3)$. These experimental and theoretical results are compared to the corresponding quantities of some similar molecules.

Introduction

Saturated five-membered ring molecules have two “out-of-plane” vibrational modes which are usually described qualitatively as ring-puckering and ring-twisting modes. When the frequencies of these two modes are nearly equal, the cross terms in the potential function give rise to a vibrational motion initially designated¹ as pseudorotation. This motion was originally treated¹ for cyclopentane for the two degenerate out-of-plane ring-bending coordinates which were written in terms of an amplitude coordinate q and a phase angle coordinate ϕ . This concept for cyclopentane was questioned² when the low frequency ring mode of this molecule appeared “normal” but the fundamentals could not be assigned on the basis that cyclopentane had D_{5h} symmetry. The authors² stated that the spectral data were consistent with a rigid structure with C_s , C_2 , or C_1 symmetry, but they² concluded that a decision among the models with pseudorotation or rigid structures could not be made. There was further reluctance^{3,4} to accept the pseudorotation of the puckering motion and the consequent indefiniteness of the cyclopentane conformation. However, a later infrared study⁵ of the CH_2 deformation of cyclopentane clearly showed

that the ring was undergoing pseudorotation which was nearly barrier free. Also from this study⁵ an estimate of the value of the pseudorotational moment⁶ of inertia was obtained from the spectral data. After the initial prediction¹ of pseudorotation in saturated five-membered rings, it was followed⁷ by a study where the authors proposed that fluorocyclopentane as well as several other five membered rings should have the bent conformation (envelope) as the preferred form. The barrier to pseudorotation for the fluoride was estimated⁷ to be 700 cal/mol (245 cm^{-1}) by employing the torsional barriers in ethane and ethyl fluoride.

Relatively complete vibrational studies^{8,9} of the cyclopentyl halides (F, Cl, Br, and I) were carried out utilizing infrared and Raman spectra, and it was concluded that the F, Cl, and Br compounds all had doublets for the carbon–halogen stretches arising from equatorial and axial conformers for the envelope form of these substituted cyclopentanes. For the chloride and bromide, the higher frequency band of the doublet which was observed in the fluid states was assigned to the equatorial conformer but it was not present in the infrared spectra of the solids. For the fluoride the doublet was reported at 978 (axial) and 985 cm^{-1} (equatorial) with the corresponding bands at 968 and 975 cm^{-1} in the liquids, respectively, but they remained in the spectra of the solids at 952 and 962 cm^{-1} but with reversed intensities with the lower-frequency band becoming significantly stronger than the higher frequency one. However, in a later vibrational study¹⁰ of fluorocyclopentane, it was reported that no evidence could be found for a second band for the CF stretch

* Corresponding author. Phone: 01 816-235-6038. Fax: 01 816-235-2290. E-mail: durigj@umkc.edu.

[†] University of Missouri—Kansas City.

[‡] College of Charleston.

[§] Taken in part from the thesis of A.M.E.D., which was submitted in partial fulfillment of the Ph.D. degree.

^{||} Taken in part from the thesis of A.G., which will be submitted in partial fulfillment of the Ph.D. degree.

and the ring twisting mode (radial mode) was a single band at 207 cm^{-1} , whereas for the corresponding chloride and bromide, this mode was clearly a doublet. Thus, it was concluded that fluorocyclopentane existed as a single stable conformer which was consistent with the predictions from CNDO/2 calculations that only the envelope-equatorial conformer was a stable form.¹¹ This result is in marked contrast to the conformational stabilities of both chlorocyclopentane and bromocyclopentane where both the envelope-axial and equatorial conformers are clearly present in the fluid phases at ambient temperature.^{8,9}

We recently determined the enthalpy difference between the two stable forms of the chloride¹² and bromide¹³ by variable temperature studies of the infrared spectra of rare gas solutions. For chlorocyclopentane¹² the enthalpy difference was determined to be $145 \pm 15\text{ cm}^{-1}$ ($1.73 \pm 0.18\text{ kJ/mol}$) with the axial form the more stable conformer, and similarly for the bromocyclopentane,¹³ the enthalpy difference is $233 \pm 23\text{ cm}^{-1}$ ($2.79 \pm 0.28\text{ kJ/mol}$) again with the more stable form the axial conformer. We have also shown from the infrared spectra of variable temperature studies of rare gas solutions of silacyclopentane¹⁴ and germacyclopentane¹⁵ that these molecules have a single stable conformer with a twisted heavy atom skeleton (C_2 symmetry). Thus, if the fluoride has only one stable conformer, it is more probable that it is the twisted form rather than only one of the envelope conformers.

Therefore, we have investigated the vibrational spectrum of fluorocyclopentane with a study of the infrared spectra of the gas, solid and xenon solutions. Additionally we have investigated the Raman spectrum of the liquid and solid. To support the vibrational study, we have carried out ab initio calculations at the MP2 level with full electron correlation by the perturbation method¹⁶ utilizing a variety of basis sets up to 6-311G(2d,2p) as well as those with diffuse functions, i.e., 6-311+G(2d,2p). We found that there is not a significant difference in the predicted stabilities of $c\text{-C}_5\text{H}_9\text{F}$ with the size of the basis set, particularly with the inclusion of diffuse functions. We also carried out density functional theory (DFT) calculations by the B3LYP method with the corresponding basis sets used for the MP2 calculations. We have calculated the optimized geometries, conformational stabilities, harmonic force fields, infrared intensities, Raman activities, and depolarization ratios. The results of these spectroscopic and theoretical studies are reported herein.

Experimental Section

The sample of fluorocyclopentane was prepared according to the method of Shellhamer et al.¹⁷ The sample was first purified by trap-to-trap distillation three times and then by a low-pressure, low-temperature sublimation column. The purity of the sample was determined by the infrared spectrum of the gas and by nuclear magnetic resonance in deuterated chloroform.

The mid-infrared spectrum of the gas (Figure 1) was obtained from 3200 to 230 cm^{-1} on a Perkin-Elmer model 2000 Fourier transform spectrometer equipped with a Ge/CsI beamsplitter and a DTGS detector. Atmospheric water vapor was removed from the spectrometer housing by purging with dry nitrogen. The theoretical resolution used to obtain the spectrum of the gas was 0.5 cm^{-1} . Sixty-four interferograms were added and truncated with a boxcar function.

The mid-infrared spectra ($3200\text{--}400\text{ cm}^{-1}$) of the sample dissolved in liquefied xenon were recorded on a Bruker model IFS-66 Fourier transform spectrometer equipped with a global source, a Ge/KBr beamsplitter and a DTGS detector. In all cases, 100 interferograms were collected at a 1.0 cm^{-1} resolution, averaged, and transformed with a boxcar truncation function.

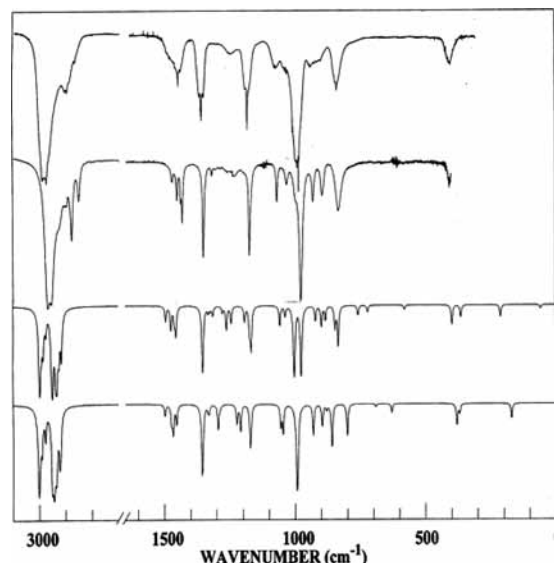


Figure 1. Comparison of experimental and calculated infrared spectra of fluorocyclopentane: (A) observed infrared spectrum in gas; (B) observed infrared spectrum in liquid xenon solution at $-95\text{ }^\circ\text{C}$; (C) simulated infrared spectrum of twisted (C_1) fluorocyclopentane; (D) simulated infrared spectrum of envelope equatorial (C_s) fluorocyclopentane.

For these studies, a specially designed cryostat cell was used which has been previously described.¹⁸

The far-infrared spectrum of the sample was recorded on the previously described Perkin-Elmer 2000 spectrometer. A grid beam splitter and a cryostat cell with polyethylene windows was used to record the spectrum of the solid with sample being deposited on a silicon substrate at 77 K, and multiple annealings were performed in order to obtain a good polycrystalline solid. For the spectrum of the gas, the sample was contained in a 12 cm cell equipped with polyethylene windows. The spectra were recorded at a spectral resolution of 0.5 cm^{-1} , and typically, 256 scans were used for both the sample and the reference data to give a satisfactory signal-to-noise ratio. The interferograms were averaged and then transformed with a boxcar truncation function.

The Raman spectra were recorded on a Spex model 1403 spectrophotometer equipped with a Spectra-Physics model 2017 argon ion laser operating on the 514.5 nm line. The laser power used was 1.5 W with a spectral bandpass of 3 cm^{-1} . The spectrum of the liquid was recorded with the sample sealed in a Pyrex glass capillary. The spectrum of the annealed solid was obtained by condensing the sample on a blackened brass block, which was maintained in a cell fitted with quartz window, cooled with boiling nitrogen and annealed until no further changes in the spectrum were noted. The measurements of the Raman frequencies are expected to be accurate to $\pm 2\text{ cm}^{-1}$. All of the bands observed in the various infrared and Raman spectra which were chosen as fundamentals are listed in Table 1.

Ab Initio Calculations

The ab initio calculations were performed with the Gaussian 03 program¹⁹ using Gaussian-type basis functions. The energy minima with respect to nuclear coordinates were obtained by the simultaneous relaxation of all geometric parameters using the gradient method of Pulay.²⁰ A variety of basis sets beginning with 6-31G(d) and up to 6-311G(2df,2pd) as well as the corresponding ones with diffuse functions were employed with the Møller–Plesset perturbation method¹⁶ to the second order (MP2(full)) as well as with the density functional theory by

TABLE 1: Calculated^a and Observed Frequencies (cm⁻¹) for Fluorocyclopentane Twisted (C₁) Form

vib. No.	approx. description	MP2/6-31G(d)	fixed scaled ^b	IR int.	Raman act.	dp ratio	IR				Raman		P.E.D. ^c	band contour		
							gas	soln	liquid	liquid	solid	solid		A	B	C
ν_1	β -CH ₂ anti sym. stretch	3197	2999	43.1	41.6	0.66	2988		0	2972	2986	2986	60S ₁ ,34S ₃	29	2	69
ν_2	α -CH ₂ anti sym. stretch	3190	2992	6.1	84.4	0.75	2978 2970	2968	2969	2976	2977	62S ₂ ,23S ₄ ,10S ₁	67	30	3	
ν_3	α -CH ₂ anti sym. stretch	3183	2986	10.0	89.3	0.47	2964 2956				2966	51S ₃ ,21S ₁ ,15S ₂	4	96		
ν_4	β -CH ₂ anti sym. stretch	3172	2976	4.2	46.7	0.51	2955			2943	2947	69S ₄ ,10S ₂	46	4	50	
ν_5	CH stretch	3146	2951	49.7	151.4	0.09	2925		2928	2916	2920	83S ₅ ,12S ₈	32	8	60	
ν_6	β -CH ₂ symmetric str.	3132	2938	27.3	105.7	0.12	2914 2904			2901		69S ₆ ,24S ₇	55	13	32	
ν_7	β -CH ₂ symmetric str.	3127	2934	28.3	45.6	0.27	2893 2895	2897	2890	2895	2880	39S ₇ ,25S ₉ ,21S ₈	26	73	1	
ν_8	α -CH ₂ symmetric str.	3119	2926	11.3	32.0	0.67	2879 2876	2875	2878	2874	2872	17S ₈ ,36S ₇ ,21S ₆ ,17S ₉	96	4	4	
ν_9	α -CH ₂ symmetric str.	3110	2917	12.3	67.3	0.26	2858 2848	2848	2858	2854	2851	45S ₉ ,41S ₈	4	35	61	
ν_{10}	β -CH ₂ deformation	1577	1496	3.0	6.9	0.61	1476 1470	1471	1476	1467	1478	80S ₁₀ ,16S ₁₂	95	3	2	
ν_{11}	β -CH ₂ deformation	1556	1476	4.9	11.0	0.75	1460 1451	1452	1442	1448	1458	88S ₁₁		60	40	
ν_{12}	α -CH ₂ deformation	1542	1463	3.1	10.7	0.74	1443 1437	1435	1439	1440	1445	81S ₁₂ ,14S ₁₀	3	0	97	
ν_{13}	α -CH ₂ deformation	1536	1457	6.1	13.8	0.75	1434 1431	1430	1436	1434	1433	93S ₁₃	1	83	16	
ν_{14}	CH in-plane bend ^d	1427	1354	20.1	1.4	0.68	1353 1350	1349	1355	1349	1349	52S ₁₄ ,13S ₂₀ ,12S ₃₇	88		12	
ν_{15}	β -CH ₂ wag	1405	1333	1.2	1.2	0.74	1332		1341	1330	1333	34S ₁₅ ,34S ₁₉ ,13S ₂₉ ,10S ₁₈	53	44	3	
ν_{16}	α -CH ₂ wag	1397	1325	0.8	0.5	0.69	1323 1319	1320	1320	1319	1321	57S ₁₆ ,13S ₁₇	35	22	43	
ν_{17}	β -CH ₂ wag	1387	1315	1.9	6.3	0.75	1307 1306	1308	1308	1305	1303	31S ₁₇ ,31S ₂₁	72	25	3	
ν_{18}	α -CH ₂ wag	1347	1278	1.3	0.7	0.75	1286 1286	1286	1273	1284	1287	49S ₁₈ ,34S ₁₅ ,10S ₁₉	1	98	1	
ν_{19}	CH out-of-plane bend ^d	1331	1263	4.9	6.0	0.74	1260 1264	1267	1267	1267	1266	12S ₁₉ ,13S ₁₅ ,12S ₂₁	20	79	1	
ν_{20}	α -CH ₂ twist	1312	1245	3.4	16.2	0.74	1246 1241	1234		1235	1237	33S ₂₀ ,21S ₂₂	13	72	15	
ν_{21}	β -CH ₂ twist	1259	1194	3.1	8.9	0.74	1199 1197	1197	1198	1199	1200	24S ₂₁ ,20S ₂₃ ,12S ₂₄ ,10S ₁₇	23	12	65	
ν_{22}	β -CH ₂ twist	1239	1175	5.2	2.9	0.75	1179 1174		1178	1174	1174	20S ₂₂ ,13S ₂₁ ,10S ₂₃		67	33	
ν_{23}	α -CH ₂ twist	1232	1169	10.2	3.9	0.71	1173	1170	1172	1164	1164	19S ₂₃ ,13S ₂₂ ,13S ₂₀ ,10S ₂₈	32		68	
ν_{24}	β -CH ₂ rock	1116	1059	4.0	7.6	0.75	1071 1069	1070	1071	1069	1069	13S ₂₄ ,18S ₁₉ ,17S ₂₆ ,13S ₁₈ ,15S ₃₃ ,14S ₂₃	91	9		
ν_{25}	ring deformation	1094	1038	2.0	7.8	0.74	1033 1032	1033	1033	1032	1037	31S ₂₅ ,25S ₃₄ ,14S ₁₇	99	1		
ν_{26}	ring deformation	1057	1003	22.6	3.8	0.71	1003 998	998	1003	996	997	10S ₂₆ ,24S ₂₇ ,14S ₂₀	35	5	60	
ν_{27}	CF stretch	1029	977	22.1	4.7	0.72	979 975	966	973	966	966	23S ₂₇ ,13S ₂₆ ,10S ₂₅ ,10S ₂₄	47		53	
ν_{28}	α -CH ₂ rock	972	922	2.9	2.5	0.19	935 931	931	930	928	929	24S ₂₈ ,12S ₃₀ ,11S ₃₄ ,10S ₂₅	32	20	48	
ν_{29}	ring deformation	948	899	4.1	2.7	0.07	910 908			900	903	40S ₂₉ ,11S ₃₄ ,11S ₃₀	3	88	9	
ν_{30}	ring breathing	932	884	2.7	11.5	0.08	895 896	897	894	895	896	44S ₃₀ ,13S ₂₉ ,10S ₃₄	51	47	2	
ν_{31}	ring deformation	893	847	4.5	3.4	0.14		852	852	852	853	19S ₃₁ ,17S ₂₈ ,13S ₂₅ ,13S ₂₇ ,10S ₃₃	4		96	
ν_{32}	β -CH ₂ rock	880	835	9.2	3.5	0.15	835 833	818	828	818	818	37S ₃₂ ,13S ₂₆ ,12S ₂₇ ,10S ₃₀	51	3	46	
ν_{33}	α -CH ₂ rock	800	759	1.9	1.2	0.27				781	781	23S ₃₃ ,21S ₃₂ ,14S ₂₉ ,11S ₂₄	67	33		
ν_{34}	ring deformation	761	722	1.3	0.8	0.37				705	708	13S ₃₄ , 18S ₃₃ , 11S ₃₇ , 32S ₃₁ , 11S ₃₅	98		2	
ν_{35}	ring deformation	612	580	0.8	0.7	0.73	582			581	584	42S ₃₅ ,26S ₃₂	27	61	12	
ν_{36}	CF out-of-plane bend ^d	420	398	3.9	0.4	0.74	404 406	407	400	416	422	65S ₃₆ ,10S ₃₅ ,10S ₃₃	4	90	6	
ν_{37}	CF in-plane bend ^d	384	364	2.3	0.2	0.64	391	390		392	392	29S ₃₇ ,20S ₃₁ ,16S ₃₈ ,13S ₃₆ ,11S ₂₈	65	33	2	
ν_{38}	ring puckering	223	211	2.2	0.0	0.72	208			246	241	25S ₃₈ ,34S ₃₉ ,21S ₃₇ ,10S ₃₁	78	16	6	
ν_{39}	ring twist	60	57	0.7	0.1	0.64	58					54S ₃₉ ,45S ₃₈	60	7	33	

^a MP2(full)/6-31G(d) ab initio calculations, scaled frequencies, infrared intensities (km/mol), Raman activities ($\text{Å}^4/\text{u}$), depolarization ratios (dp), and potential energy distributions (P.E.D.s). ^b Scaled frequencies with scaling factors of 0.88 for CH stretch and 0.90 for all other modes. ^c Symmetry coordinates with PED contribution less than 10% are omitted. ^d Pseudoplane of the ring.

the B3LYP method with the same basis sets. The predicted conformational energy differences are listed in Table 2.

In order to obtain a complete description of the molecular motions involved in the fundamental modes of fluorocyclopentane, a normal coordinate analysis has been carried out. The force field in Cartesian coordinates was obtained with the Gaussian 03 program at the MP2(full) level with the 6-31G(d) basis set. The internal coordinates used to calculate the **G** and **B** matrices are given in Table 3 with the atomic numbering shown in Figure 2. By using the **B** matrix,²¹ the force field in Cartesian coordinates was converted to a force field in internal coordinates. Subsequently, scaling factors of 0.88 for CH stretches, and 0.90 for all other coordinates were applied, along with the geometric average of scaling factors for interaction force constants, to obtain the fixed scaled force field and resultant wavenumbers. A set of symmetry coordinates was used (Table 1S) to determine the corresponding potential energy distributions (P.E.D.s). A comparison between the observed and calculated wavenumbers, along with the calculated infrared

intensities, Raman activities, depolarization ratios and potential energy distributions for twisted fluorocyclopentane are listed in Table 1.

The infrared spectra were predicted from the MP2(full)/6-31G(d) calculations. The predicted scaled frequencies were used together with a Lorentzian function to obtain the calculated spectra. Infrared intensities determined from the MP2(full)/6-31G(d) calculations were obtained based on the dipole moment derivatives with respect to Cartesian coordinates. The derivatives were transformed with respect to normal coordinates by $(\partial\mu_{ij}/\partial Q_i) = \sum_j(\partial\mu_{ij}/\partial X_j)\mathbf{L}_{ij}$, where Q_i is the i th normal coordinate, X_j is the j th Cartesian displacement coordinate, and \mathbf{L}_{ij} is the transformation matrix between the Cartesian displacement coordinates and the normal coordinates. The infrared intensities were then calculated by $N\pi/3c^2 [(\partial\mu_{ij}/\partial Q_i)^2 + (\partial\mu_{ij}/\partial Q_j)^2 + (\partial\mu_{ij}/\partial Q_k)^2]$. In Figure 1, a comparison of experimental and simulated infrared spectra of fluorocyclopentane is shown. The predicted spectrum for the twisted form is in good agreement with the experimental spectrum which indicates the utility of the scaled

TABLE 2: Calculated Electronic Energies (hartree) and Energy Differences (cm⁻¹) for the Twisted C₁, Planar C_s, and Envelope C_s of Fluorocyclopentane

method/basis set	twisted (C ₁) <i>E_n</i> ^a	energy difference (cm ⁻¹) ^b		
		envelope (C _s)		planar (C _s)
		axial	equatorial	
MP2(full)/6-31G(d)	0.865656	44	752*	2600
MP2(full)/6-31+G(d)	0.887704	27	726	2390
MP2(full)/6-311G(d,p)	1.152336	128	672	2493
MP2(full)/6-311+G(d,p)	1.162450	78	640	2398
MP2(full)/6-311G(2d,2p)	1.236825	106	742	2650
MP2(full)/6-311+G(2d,2p)	1.244533	56	691	2562
MP2(full)/6-311G(2df,2pd)	1.340861	115	679	
MP2(full)/6-311+G(2df,2pd)	1.348131	66	639	2567
MP2(full)/6-311++G(2df,2pd)	1.348509	76	646	
MP2(full)/aug-cc-pVTZ	1.365720	49	641	
Average of MP2(full) predictions		75 ± 33	683 ± 44	2523 ± 100
B3LYP/6-31G(d)	1.791518	76	466	1907
B3LYP/6-31+G(d)	1.809498	50	504	1713
B3LYP/6-311G(d, p)	1.878374	91	547	1816
B3LYP/6-311+G(d,p)	1.885182	46	512	1708
B3LYP/6-311G(2d,2p)	1.889874	106	572	1742
B3LYP/6-311+G(2d,2p)	1.895666	49	524	1670
B3LYP/6-311G(2df,2pd)	1.896371	104	524	
B3LYP/6-311+G(2df,2pd)	1.902222	55	498	
B3LYP/6-311++G(2df,2pd)	1.902231	36	482	
B3LYP/aug-cc-pVTZ	1.912003	46	483	
average of B3LYP predictions		66 ± 26	511 ± 32	1759 ± 87

^a Energy of twisted (C₁) conformer is given as $-(E + 294)H$. ^b Energies of conformations relative to the twisted C₁ conformer. Envelope forms are first order saddle points, except the one marked with asterisk.

predicted frequencies and predicted intensities for supporting the vibrational assignment and the conformational conclusion.

Also to further support the vibrational assignments, we have simulated the Raman spectra from the ab initio MP2(full)/6-31G(d) results. The evaluation of Raman activity by using the analytical gradient methods has been developed.^{22–25} The activity S_j can be expressed as: $S_j = g_j(45\alpha_j^2 + 7\beta_j^2)$, where g_j is the degeneracy of the vibrational mode j , α_j is the derivative of the isotropic polarizability, and β_j is that of the anisotropic polarizability. To obtain the polarized Raman scattering cross sections, the polarizabilities are incorporated into S_j by multiplying S_j with $(1 - \rho_j)/(1 + \rho_j)$, where ρ_j is the depolarization ratio of the j th normal mode. The Raman scattering cross sections and calculated wavenumbers obtained from the Gaussian 03 program were used together with a Lorentzian function to obtain the simulated Raman spectra. Comparison of experimental Raman spectrum of the liquid, the predicted one and the spectrum of the solid are shown in Figure 3A–C, respectively.

It should be noted that three of the predicted Raman “doublets” in the region from ~350 to 900 cm⁻¹ appear as two single bands at 400 and 828 cm⁻¹ with the third one not appearing. The lower frequency doublet is due to the two CF bending modes whereas the higher frequency one is due to two ring modes. However in the Raman spectrum of the solid these doublets are clearly observed. Therefore the comparison of the Raman spectrum of the liquid and solid gives some qualitative indication that the molecule is undergoing pseudorotation in the fluid phases with a very small barrier.

Conformational Stability and Structural Parameters

To investigate the possibility that fluorocyclopentane has a second stable conformer the temperature dependent infrared spectra of the sample was recorded as a very dilute solution in liquid xenon at -65 and -95 °C. A portion of these spectra at these temperatures is shown in Figure 4 and there is no

indication of any relative changes in the band intensities. There is a decrease in the bandwidths of most of the absorption bands and the fundamental at 998 cm⁻¹ (ν_{26}) and the ν_{27} fundamental at 975 cm⁻¹ become more pronounced at the lower temperature but there is no indications of a second CF stretching mode which would be expected if a second conformer were present. The frequency for the CF stretch was predicted for the envelope-axial form at 993 cm⁻¹ (intensity 35.6 km/mol) and for the envelope-equatorial at 1072 cm⁻¹ (intensity 77.7 km/mol) which was previously proposed as the only stable conformer.^{10,11} For the twisted C₁ form the predicted CF stretch (ν_{27} ; 979 cm⁻¹) is extensively mixed with ν_{26} (1003 cm⁻¹; ring deformation) with the predicted intensities of 22.1 and 22.6 km/mol, respectively, where the observed frequencies are within 2 cm⁻¹ of the predicted values (Table 1). Therefore, if there was even a very small amount of the envelope-equatorial form present in the fluid phases it should be detectable based on the predicted frequency and intensity of the CF stretch where the predicted frequency is expected to be within a few cm⁻¹, i.e., better than ± 10 cm⁻¹.

A comparison of the infrared spectrum of the gas with the one of the xenon solution shows the complex spectrum of the gas is probably due to “hot bands” rather than fundamentals of a second conformer. In the spectral region from 800 to 1075 cm⁻¹, the infrared spectrum of the gas is quite complex (Figure 5), but the spectrum in the xenon solution is well accounted for by a single conformer. Only the gas phase band at 895 cm⁻¹ which has a significant amount of absorption to higher frequency is due to two bands and one of them the lower frequency mode is obviously the ring breathing fundamental which gives rise to a very strong Raman line (Figure 3). The second one at ~910 cm⁻¹ can confidently be assigned as ν_{25} , the ring deformation, which is clearly observed in the Raman spectrum of the solid. Another band at 931 cm⁻¹ (xenon; 935 cm⁻¹ in the gas) which contributes to the absorption in this region has been ap-

TABLE 3: Structural Parameters (Å and degree), Rotational Constants (MHz), and Dipole Moment (debye) for Fluorocyclopentane Twisted (C_1) and Envelope Axial and Equatorial (C_s) Forms

structural parameters	internal coordinates	ab initio MP2(full)/6-311+G(d,p)				adjusted r_0 for the twisted ^c C_1
		envelope (C_s) ^b			twisted (C_1) ^a	
		axial	equatorial	twisted		
$r(C_1-C_2)$	X_1	1.529	1.517	1.519	1.531(3)	
$r(C_1-C_3)$	X_2	1.518	1.517	1.519	1.519(3)	
$r(C_2-C_4)$	Y_1	1.551	1.542	1.539	1.553(3)	
$r(C_3-C_5)$	Y_2	1.531	1.542	1.539	1.533(3)	
$r(C_4-C_5)$	Z	1.539	1.554	1.559	1.540(3)	
$r(C_1-F_6)$	r_1	1.408	1.406	1.395	1.411(3)	
$r(C-H_7)$	r_2	1.092	1.093	1.096	1.092(2)	
$r(C-H_8)$	r_3	1.092	1.092	1.095	1.092(2)	
$r(C-H_9)$	r_4	1.097	1.096	1.092	1.097(2)	
$r(C-H_{10})$	r_5	1.094	1.096	1.092	1.094(2)	
$r(C-H_{11})$	r_6	1.092	1.092	1.095	1.092(2)	
$r(C-H_{12})$	r_7	1.094	1.092	1.092	1.094(2)	
$r(C-H_{13})$	r_8	1.095	1.093	1.094	1.095(2)	
$r(C-H_{14})$	r_9	1.093	1.093	1.094	1.093(2)	
$r(C-H_{15})$	r_{10}	1.092	1.092	1.092	1.092(2)	
$\angle C_3C_1C_2$	θ	105.1	103.8	103.5	105.5(5)	
$\angle C_1C_2C_4$	ψ_1	105.9	104.0	103.0	106.2(5)	
$\angle C_1C_3C_5$	ψ_2	102.5	104.0	103.0	102.9(5)	
$\angle C_2C_4C_5$	φ_1	105.2	105.7	105.6	105.3(5)	
$\angle C_3C_5C_4$	φ_2	103.1	105.7	105.6	104.6(5)	
$\angle F_6C_1H_7$	α	106.4	106.8	106.8	106.2(5)	
$\angle H_8C_2H_{10}$	γ_1	107.6	108.2	108.3	107.6(5)	
$\angle H_9C_3H_{11}$	γ_2	108.7	108.2	108.3	108.7(5)	
$\angle H_{12}C_4H_{14}$	ϵ_1	108.1	107.4	107.0	108.1(5)	
$\angle H_{13}C_5H_{15}$	ϵ_2	107.4	107.4	107.0	107.4(5)	
$\angle F_6C_1C_2$	β_1	108.7	108.4	112.1	108.9(5)	
$\angle H_7C_1C_3$	β_4	114.6	114.6	111.2	114.6(5)	
$\angle F_6C_1C_3$	β_2	107.8	108.4	112.1	107.6(5)	
$\angle H_7C_1C_2$	β_3	114.0	114.6	111.2	113.8(5)	
$\angle H_8C_2C_1$	π_1	109.0	111.9	107.5	109.0(5)	
$\angle H_9C_3C_1$	π_5	108.7	108.2	113.3	108.7(5)	
$\angle H_{10}C_4C_1$	π_3	110.0	108.2	113.3	110.0(5)	
$\angle H_{11}C_5C_1$	π_7	111.8	111.9	107.5	111.8(5)	
$\angle H_8C_2C_4$	π_2	112.9	113.6	111.0	112.7(5)	
$\angle H_9C_3C_5$	π_6	110.2	110.9	113.6	110.0(5)	
$\angle H_{10}C_4C_2$	π_4	111.5	110.9	113.6	111.3(5)	
$\angle H_{11}C_5C_5$	π_8	114.7	113.6	111.0	114.5(5)	
$\angle H_{12}C_5C_4$	σ_6	110.3	110.2	112.1	109.6(5)	
$\angle H_{13}C_4C_5$	σ_2	109.7	112.1	110.3	109.6(5)	
$\angle H_{14}C_5C_4$	σ_8	112.7	112.1	110.2	111.8(5)	
$\angle H_{15}C_4C_5$	σ_4	112.4	110.2	112.1	112.3(5)	
$\angle H_{12}C_5C_3$	σ_5	109.3	110.0	111.5	109.3(5)	
$\angle H_{13}C_4C_2$	σ_1	109.9	111.4	110.3	109.9(5)	
$\angle H_{14}C_5C_3$	σ_7	113.3	111.4	110.3	113.3(5)	
$\angle H_{15}C_4C_2$	σ_3	112.3	110.0	111.5	112.3(5)	
$\tau(C_1C_2C_4C_5)$	τ_1	-6.4	24.2	-25.6	-2.6(3)	
$\tau(C_2C_4C_5C_3)$	τ_2	30.0	0.0	0.0	25.3(3)	
A		5284	5011	6500	5257	
B		3481	3601	2980	3462	
C		2776	2920	2242	2753	
$ \mu_a $		1.579	1.387	2.379		
$ \mu_b $		0.156	0.000	0.000		
$ \mu_c $		1.571	1.739	0.477		
$ \mu_d $		2.233	2.224	2.426		

^a Values taken from MP2(full)/6-311+G(d,p) calculations.

^b Saddle points. ^c Experimental rotational constants: A = 5256.55(5), B = 3460.95(5), C = 2753.53(4) MHz.²⁶

proximately described as a α -CH₂ rock (24% S_{28}) but it has 12, 11, and 10% contributions from three ring modes (Table 1) as well as ~7% contributions from the CF bend and two CH₂ bends. In going from the gas to the liquid (Figure 6B) essentially the same bands are observed as those observed in the xenon solution but with a significant frequency shift of the band assigned to the CF stretch. With repeated annealing (Figure 6C and 6D) no band disappears as would be expected if a second conformer were present in the liquid. In fact instead of a band

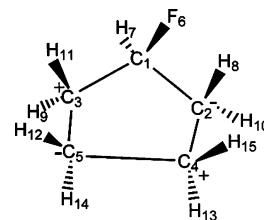


Figure 2. Twisted conformer of fluorocyclopentane showing atomic numbering.

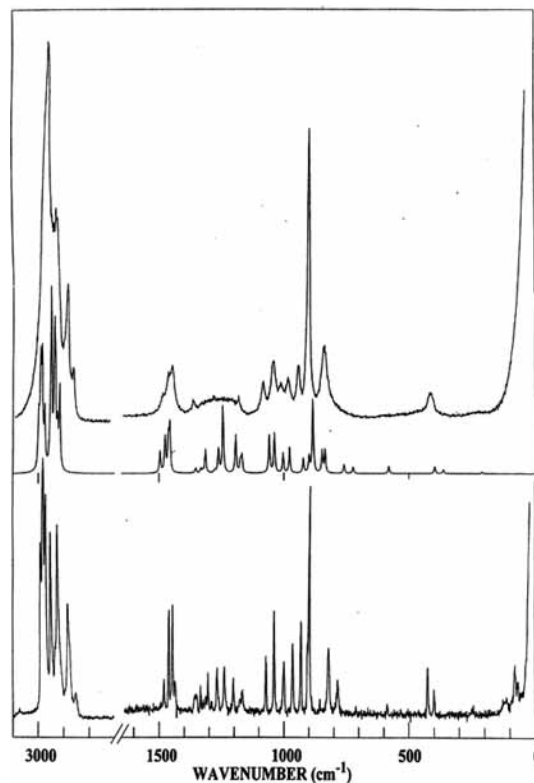


Figure 3. Raman spectra (0–3100 cm⁻¹) of fluorocyclopentane: (A) liquid, (B) simulated spectrum from MP2(full)/6-31G(d) calculations, and (C) solid.

disappearing, significant new bands appear in the spectra of the condensed phases. The infrared band at 835 cm⁻¹ with a well-defined band contour in the gas becomes a very broadband in the liquid with a very pronounced broad low frequency shoulder (Figure 6B). In the infrared spectrum of the solid the band splits into the three relatively sharp bands at 852, 818, and 781 cm⁻¹ which are ν_{31} , ν_{32} , and ν_{33} , respectively. All three modes are extensively mixed with the major contributions from the CH₂ rocks and ring deformations. Also of interest are ν_{34} and ν_{35} which have major contributions from two ring deformations which are pronounced bands at 705 and 581 cm⁻¹ in the spectrum of the solid but not observed in the spectra of the gas and liquid except possibly the very broad nondescript absorption in the general areas of the two fundamentals. These extremely broad bands for the ring modes are undoubtedly due to the large amplitude ring motions of the five-membered ring with a very, very low barrier to pseudorotation. Thus, all of the experimental data indicate that there is only one conformer present in the fluid phases which has a very large amplitude pseudorotation motion at and below ambient temperature.

With the conclusion that there is a single conformer in all phases, the question is raised what observation led the earliest investigators⁹ to conclude that there is a second conformer for

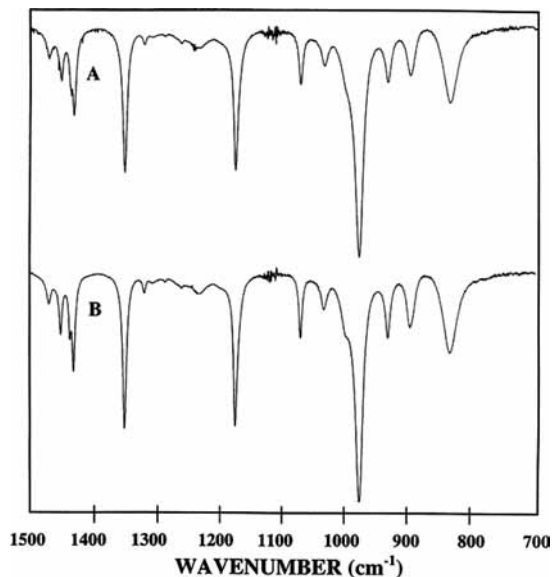


Figure 4. Midinfrared spectra ($700\text{--}1500\text{ cm}^{-1}$) of fluorocyclopentane: (A) liquid xenon solution at $-65\text{ }^{\circ}\text{C}$ and (B) liquid xenon solution at $-95\text{ }^{\circ}\text{C}$.

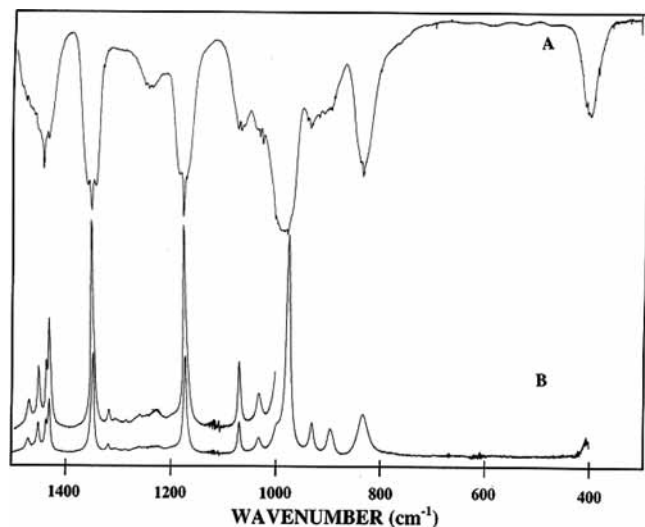


Figure 5. Midinfrared spectra ($400\text{--}1500\text{ cm}^{-1}$) of (A) gas in transmittance and (B) liquid xenon solution at $-95\text{ }^{\circ}\text{C}$ in absorbance for fluorocyclopentane.

fluorocyclopentane in the fluid phases. It appears that the “behavior” of the infrared spectral changes from the gas at ambient temperature to the liquid (21 and $-78\text{ }^{\circ}\text{C}$) and then to the solid ($-150\text{ }^{\circ}\text{C}$) over the frequency range of $850\text{--}1100\text{ cm}^{-1}$ was the reason the earliest investigators⁹ concluded there were two forms present in the fluid phases. Thus, we investigated the same region and observed some of the same changes which we believe are due to nearly potential free pseudorotation in the fluid phases with a fixed twisted (C_1) form in the solid state. However, we found many changes which were not previously reported. For example, there are relative changes of the bands with repeated annealing of the solid (Figure 6D) and some pronounced bands appear in the solid which are not observed in any of the infrared spectra of the gas, rare gas solution, or the liquid. The spectrum of the solid is significantly different from those from the fluid phases with a very pronounced band at 781 cm^{-1} which has not been previously reported.⁹ No significant shifting of the observed bands from the other phases can account for this new observed absorption. Also the region

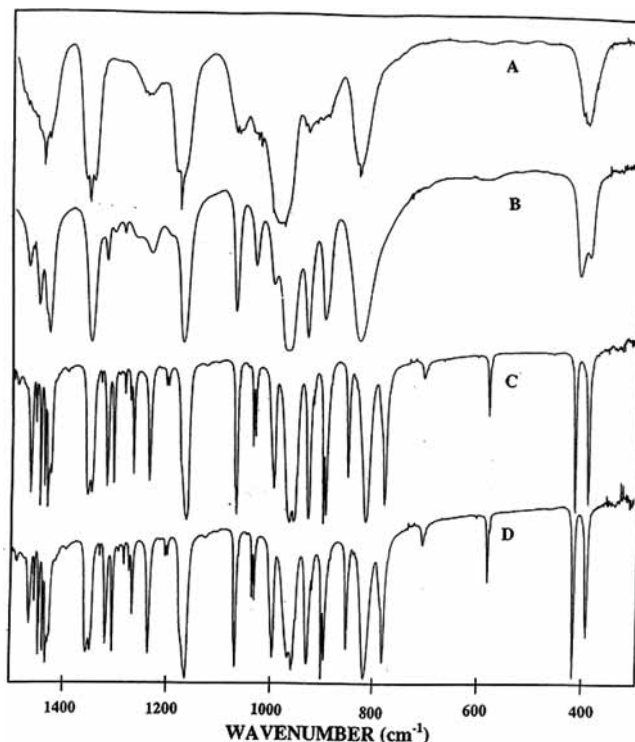


Figure 6. Midinfrared spectra ($400\text{--}1000\text{ cm}^{-1}$) of (A) gas, (B) liquid, (C) amorphous, and (D) annealed solid of fluorocyclopentane.

of the spectrum where the CF stretch is assigned shows some very interesting changes with a significant increase in the intensity of the 998 cm^{-1} band and a splitting of the 975 cm^{-1} band with shifts to lower frequencies of 966 and 962 cm^{-1} (solid). It should be noted that the earliest investigators⁹ did not record the Raman spectrum of the solid but if they had these data it is very probable they may have come to a different conclusion from the presence of two conformers. Similarly in the more recent Raman study¹⁰ only the spectrum of the liquid was recorded.

Rather conclusive evidence has recently been obtained for the identification of one conformer present in the gas from the values of the microwave determined²⁶ rotational constants. We²⁷ have found that the MP2(full)/6-311+G(d,p) ab initio calculation predicted the r_0 structural parameters for more than 50 carbon–hydrogen distances within 0.002 \AA to the experimentally determined values. The parameters utilized for comparison were those determined from “isolated” CH stretching frequencies which were compared²⁸ to previously determined r_0 values from earlier microwave studies. Additionally these calculations predict carbon–carbon distances r_0 within a few thousands of an angstrom. A large number of CF distances have been predicted and compared to the experimentally determined values²⁹ and again at this ab initio level and basis set distances to an average of better than 0.003 \AA for 20 molecules were predicted.

Based on this information the predicted rotational constants from the MP2(full)/6-311+G(d,p) calculations should predict all three of the rotational constants within about 30 MHz. As can be seen from the data listed in Table 3, the envelope-equatorial form has rotational constants with differences of 1243, 480, and 511 MHz for A, B, and C, respectively, from the experimental values and those for the envelope-axial form have differences of 245, 140, and 167 MHz for A, B, and C, respectively. However the rotational constant differences²⁶ are only 28, 20, and 23 MHz for A, B, and C, respectively, for the twisted conformer of C_1 symmetry which is clear evidence that

the conformer in the gas phase is the twisted form. This conclusion is in agreement with the predicted conformational stability from the *ab initio* calculations.

It should be possible to obtain very good structural parameters by utilizing the carbon–hydrogen parameters from the MP2(full)/6-311+G(d,p) calculations and very minor adjustments of the heavy atom parameters to fit the experimentally determined rotational constants. The values for all of the parameters are listed in Table 3, and it can be seen that only very, very small adjustments (average of 0.002 Å) were needed to fit the rotational constants. It is believed that these heavy atom distances are accurate to 0.003 Å and the CH distances to 0.002 Å. The angles are expected to be accurate to $\pm 0.5^\circ$. With these parameters it should be possible to predict the rotational constants for the ^{13}C isotomers and assign the microwave spectrum from the naturally occurring abundance of these isotomers.

Discussion

In the spectroscopic studies of Ekejiuba and Hallam,⁸ no attempt was made to provide a complete vibrational assignment for fluorocyclopentane, but the reported infrared bands for the vapor and liquid numbered 19 and 24, respectively, with only 13 of them assigned. The descriptions were quite general with only three of them designated as heavy atom ring modes. However, in the later study of Wertz and Shasky,¹⁰ all nine of the ring modes were assigned from the Raman spectrum of the liquid with similar bands in the infrared spectrum. One of these assignments of a ring mode at 525 cm^{-1} seems in error since there is only one fundamental predicted to fall in the 500 to 700 cm^{-1} region and it is clearly the band at 582 cm^{-1} which is the ring mode in this region and it was previously assigned also as a ring mode. Our comparable vibrational assignment of this ring mode is a band near 900 cm^{-1} . The infrared band of the gas in this region from 870 to 945 cm^{-1} is very complex with many maxima and the complexity is undoubtedly due to the pseudorotation of the ring. Moreover the breadth of the 896 cm^{-1} band in the infrared spectrum of the xenon solution indicates a second band near this frequency. Also the *ab initio* predictions indicate there are three ring modes in this region. Our assignments for the other eight ring modes agree with these previously proposed¹⁰ values.

There is another region of the Raman spectrum, *i.e.*, 1100–1350 cm^{-1} , which shows extensive generalized scattering in the liquid, which becomes very definitive in the spectrum of the solid. There are 10 fundamentals predicted in this region and they are CH_2 bending modes which again are drastically affected by the pseudorotation. In the infrared spectrum of the gas there is one pronounced band centered at 1246 cm^{-1} with a clear, broad absorption on the high frequency side. However distinct maxima are observed in the infrared spectrum of the xenon solution (Figure 5), and most of these bands have corresponding ones in the Raman spectrum of the solid. Assignments of these fundamentals were made mainly from the data from the xenon solution and the Raman spectrum of the solid. Finally it should be noted that the predicted infrared band contours and Raman depolarization values were not as helpful in making the vibrational assignment as usually found. However the calculated frequencies from the MP2(full)/6-31G(d) calculations with two scaling factors predicted the fundamentals for substituted hydrocarbons to within an average of 10 cm^{-1} (better than 1%) so the assignment given herein is expected to be as good as can be obtained for the fluorocyclopentane molecule.

The mixing of the CH_2 motions with the ring modes is much greater than normally found. For some of the fundamentals in the “finger print” region, the total P.E.D.s have only 60% of the indicated vibrational motion or even less, but we limited the listed ones to 10% or larger contributions. For these modes there may be as many as 10 symmetry coordinates contributing 3–5% to the mode. Nevertheless the appropriate descriptions provided compare favorably with those given for some other substituted cyclopentane molecules.

The infrared spectrum of the gas is dominated by the effect of a very small barrier to pseudorotation where exceedingly broad nondescript band contours are observed for the 1003–1033 and 850–900 cm^{-1} bands which are due to modes with significant contributions from five of the ring deformational vibrations. Also the bands for the next two lower frequency ring deformations are not observed in the infrared spectrum of the gas. These bands are similar to those observed for organoisothiocyanates where the $\angle\text{CNCS}$ is very large ($\sim 150^\circ$) with a very small barrier to linearity, and the in-plane and out-of-plane angle bends give rise to a very broad ($>100 \text{ cm}^{-1}$) nondescript contour, but in the solid state they are separated by 200 cm^{-1} . Therefore, the potential function governing the ring deformations is nearly 5-fold, but the analogous potentials for the slightly different conformers with pseudorotation will have small differences in their fundamental frequencies. It should be noted that there is extensive mixing of the CH_2 rocks with the ring deformations. The approximate simple descriptions given for the fundamentals in Table 1 are more for counting purposes than for naming the molecular motions in several cases. As an example, the out-of-plane CH bend (ν_{19}) has contributions of only three symmetry coordinates with more than 10% with the highest only 13%. Another example is ν_{24} which has contributions from six symmetry coordinates but the highest contribution is only 18% which is from the CH out-of-plane bend. The band at 979 cm^{-1} has been described as the CF stretch and its infrared intensity clearly indicates that this band has a major contribution from this motion although the band at 1003 cm^{-1} is predicted to have a similar intensity. However, the experimentally observed intensity is about one-tenth the predicted intensity. Therefore, for a few of the bands, the *ab initio* predicted infrared intensities are quite poor. Nevertheless, a predominance of the predicted intensities is quite good which significantly aids the vibrational assignment.

The predicted intensities of the Raman lines are usually substantially poorer than those for the infrared bands. This is true for the Raman spectrum of the fluorocyclopentane (Figure 3), but part of the problem arises from the very broad bands for many of the ring deformations. However the ring breathing motion is not significantly broadened by the pseudorotation so its predicted intensity is consistent with the observed intensity. However, the ring deformation at $\sim 1000 \text{ cm}^{-1}$ gives rise to a very broad Raman line and those for the two lower frequency deformations¹⁰ at ~ 705 and $\sim 588 \text{ cm}^{-1}$ are so broad that the bands are hard to identify and the centers have to be estimated (Figure 3).

The lowest frequency ring modes are predicted at 211 and 57 cm^{-1} with observed bands at 208 and 58 cm^{-1} in the infrared spectrum of the gas (Figure 7). The higher frequency band is quite broad and similar breadth is observed for the corresponding Raman lines (Figure 3). The 208 cm^{-1} band is usually described as the ring puckering vibration or the radial mode for the molecule with pseudorotation. The PED indicates a large contribution of the CF in-plane bend whereas the lower frequency ring twisting motion (pseudorotational mode) has

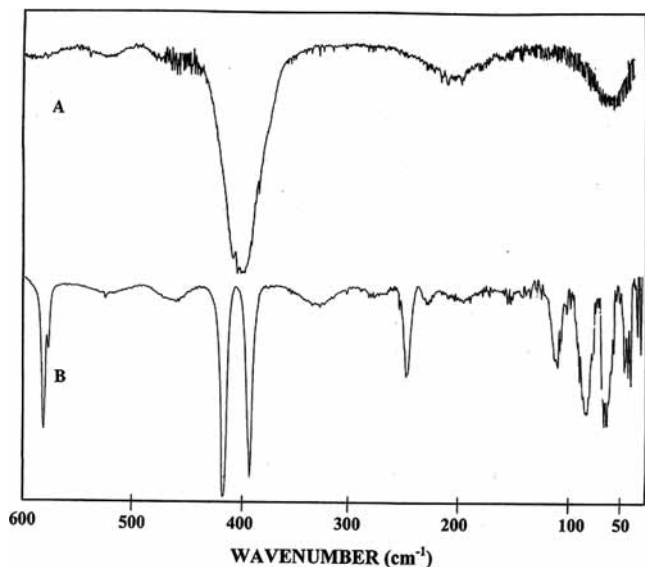


Figure 7. Far-infrared spectra (30–600 cm^{-1}) of (A) gas and (B) annealed solid of fluorocyclopentane.

nearly equal contributions from both of the two low frequency motions. In the infrared spectrum of the solid, ν_{38} shifts to 246.5 cm^{-1} with a much weaker lower frequency band at 227.5 cm^{-1} which could be a second component of ν_{38} or a two phonon band of a lattice mode. The ν_{39} fundamental seems to be mixed in the spectra of the solid with lattice modes having frequencies of 107.9, 81.5, 63.7, and 44.7 cm^{-1} for these phonon bands. Many of the fundamentals in the mid-infrared spectrum of the solid are doublets which indicate that there appears to be at least two molecules per primitive crystal cell.

There is very limited structural data available on the heavy atom parameters for monosubstituted cyclopentanes. After several structural investigations of chlorocyclopentane¹² and bromocyclopentane,¹³ reasonably consistent parameters have been obtained. With these two halogens there are two stable conformers (equatorial and axial) of the envelope form with the axial conformer the more stable form. Because of the C_s symmetry for the chloride and bromide, there are only three different CC distances in the ring where the corresponding ones for the chloride and bromide are nearly the same. However for the fluoride the C_1C_2 and C_1C_3 distances have significantly different values with the C_1C_2 somewhat shorter and the C_1C_3 distance longer than the values for this distance for the other two halides. An electron diffraction investigation of cyclopentyl silane³⁰ has been reported and it was concluded that the stable conformers were the envelope-axial and envelope-equatorial with the equatorial form more stable.

The earlier conclusions⁹ that fluorocyclopentane exists as envelope-axial and envelope-equatorial or as a single envelope-axial form^{10,11} have been shown to be wrong. There is a single conformer for fluorocyclopentane, but it is the twisted C_1 form and not the envelope form. The determined single conformer of fluorocyclopentane of the twisted form is quite surprising since the structure proposed by the three previous investigators^{8–11} did not even consider the possibility of the C_1 form. This possible oversight can be rationalized due to the fact that both chloro- and bromocyclopentane clearly were shown to have the equatorial and axial conformations as the stable forms. Additionally there have been two theoretical predictions^{7,31} that fluorocyclopentane would have the envelope as the stable conformer.

Pitzer and Donath⁷ proposed the formula: $\Delta V_c = 1.45(V_{12} - 2800)$ cal/mol, for predicting the energy difference between the envelope and twisted forms of monosubstituted cyclopentanes, where 2800 cal/mol (980 cm^{-1}) was taken from the V_3 value of the CC torsion of thiacyclopentane³² and V_{12} is the torsional barrier of the C_1C_2 or C_1C_3 bonds. The pseudorotation function of monosubstituted cyclopentanes may be considered as the summation of the torsional energy of its five ring torsions, and each torsional energy may be expressed as a series of cosine functions as proposed by Kilpatrick et al.¹ The equation originally proposed is $\Delta V_c = 1.45V_{12} - 0.55V_{24} - 0.91V_{45}$, where $V_{12} = V_{13}$, $V_{35} = V_{24}$, and V_{45} is the unique CC barrier. This equation is applicable if one only wants to calculate the energy difference between the envelope (C_s) and twist (C_2) forms, because the pseudorotation of the cyclopentane ring is basically potential free. Thus, one only needs to consider the perturbation from the replacement of the α -H atom by the substituted group, i.e., fluorine in this case. It is obvious that only the torsional functions τ_1 and τ_3 change, whereas the other three torsional functions may be considered as unchanged. Thus, the equation proposed by Kilpatrick et al.¹ reduces to the form as given by Pitzer and Donath.⁷

In the initial prediction of the energy difference for fluorocyclopentane by Pitzer and Donath,⁷ the V_{12} value was substituted from the barrier of 3306 cal/mol (1156 cm^{-1}) to internal rotation of ethyl fluoride,³³ which yielded the positive value of 0.7 kcal/mol (245 cm^{-1}) for fluorocyclopentane which indicates the envelope form. However, this model has a limitation, since it only provides the predicted energy difference between the envelope and twisted forms. Thus, if the envelope is the more stable form it does not predict whether the envelope-equatorial or envelope-axial forms is the more stable conformer. Of course this model does not take into account any repulsive steric hindrance which could have a significant effect on the conformer stability. The limitation on predicting the axial or equatorial form for the envelope conformer can be addressed by utilizing a model where more potential terms (such as the V_1 , V_2 , and V_3 terms) are utilized for calculating the energy difference, as demonstrated previously.³¹ By including more potential terms the equation for predicting the energy difference changes to the following form $\Delta V_n = V_n(\text{CH}_3\text{CH}_2-\text{CH}_2\text{X}) - V_n(\text{CH}_3\text{CH}_2-\text{CH}_3)$, which should provide a better prediction for the energy difference. In the above equation only the V_3 term is applicable for $\text{CH}_3\text{CH}_2-\text{CH}_3$ i.e., $V_3 = 3257$ cal/mol (1139 cm^{-1}),³⁴ whereas for the fluoride $\Delta V_n = V_n(\text{CH}_3\text{CH}_2-\text{CH}_2\text{X})$ will have at least three terms. Thus, this new approach can now be utilized to make the prediction for the energy differences between the envelope-equatorial and envelope-axial conformers as well as provide a prediction whether the envelope or twisted form is more stable. By utilizing this model a positive V_1 or V_2 (especially V_2) favors the equatorial form for the envelope conformer whereas a negative V_1 or V_2 favors the axial form for the envelope conformer. A positive ΔV_3 predicts the envelope conformer more stable, whereas a negative ΔV_3 predicts the twisted form as the more stable conformer.

This model was used earlier³¹ for fluorocyclopentane where an “effective” V_3 potential term for propane was used which has a V_3 value³⁴ of 3257 cal/mol (1139 cm^{-1}). For the 1-fluoropropane molecule the V_1 , V_2 , and V_3 potential terms are 346 cal/mol (121 cm^{-1}), -726 cal/mol (-254 cm^{-1}), and 3823 cal/mol (1337 cm^{-1}), respectively. The ΔV_3 is a positive 566 cal/mol (198 cm^{-1}) which indicates that the envelope conformer is the more stable form and the negative V_2 term indicates the envelope-axial is more stable than the envelope-equatorial form.

Thus, this model predicts the envelope conformer as the most stable form of fluorocyclopentane with a barrier to pseudorotation of 566 cal/mol (198 cm^{-1}) both of which are at variance with the experimentally determined values. The V_3 term as the CH_2CHF barrier is too large, but a more realistic value for this barrier could be the one obtained for ethyl fluoride³³ which is 3306 cal/mol (1156 cm^{-1}), or alternatively, the V_3 barrier for propane might be considered too small. However, there have been three different determinations of its value with $3325 \pm 20\text{ cal/mol}$ ($1163 \pm 7\text{ cm}^{-1}$)³⁵ from microwave splittings, $3294 \pm 10\text{ cal/mol}$ ($1152 \pm 3\text{ cm}^{-1}$)³⁶ again from microwave results, and the value from the infrared data.³⁴ Therefore, it seems reasonable to use the V_3 barrier from propane along with the barrier from ethyl fluoride to obtain the barrier to pseudorotation of fluorocyclopentane. By using these data a predicted barrier to pseudorotation of 28 cal/mol (9 cm^{-1}) is obtained which is consistent with the very low barrier obtained experimentally as well as the ab initio predicted value of $214 \pm 94\text{ cal/mol}$ ($75 \pm 33\text{ cm}^{-1}$).

We have utilized this newer model to predict the stability of the conformers for methylcyclopentane, where the V_3 terms for propane and ethane were used which gave a predicted barrier to pseudorotation of -575 cal/mol (201 cm^{-1}), which indicates the twisted form (C_1) to be the more stable conformer. These results are quite different from the value obtained by Pitzer and Donath⁷ of 900 cal/mol (315 cm^{-1}) by the earlier model which predicts the envelope (C_s) form to be the more stable conformer. Therefore, it would be of interest to determine the most stable conformer of methylcyclopentane. It is our assessment that the model which we propose may be effective in providing the correct prediction for the order of stability of many monosubstituted cyclopentane derivatives. Further investigations of several monosubstituted cyclopentanes are desirable both experimentally and theoretically in order to ascertain the most important factor(s) determining the stable conformers for the monosubstituted cyclopentane derivatives.

Acknowledgment. J.R.D. acknowledges the University of Missouri—Kansas City for a Faculty Research Grant for partial financial support of this research.

Supporting Information Available: Symmetry coordinates of fluorocyclopentane (Table S1). This material is available free of charge via the Internet at <http://pubs.acs.org>.

References and Notes

- (1) Kilpatrick, J. E.; Pitzer, K. S.; Spitzer, R. *J. Am. Chem. Soc.* **1947**, *69*, 2483.
- (2) Miller, F. A.; Inskip, R. G. *J. Chem. Phys.* **1950**, *18*, 1519.
- (3) Le Fevre, C. G.; Le Fevre, R. J. W. *J. Chem. Soc.* **1956**, 3549.
- (4) Curnutte, B.; Shaffer, W. F. *J. Mol. Spectrosc.* **1957**, *1*, 239.
- (5) Durig, J. R.; Wertz, D. W. *J. Chem. Phys.* **1968**, *49*, 2118.
- (6) Harris, D. O.; Engerholm, G. G.; Tolman, C. A.; Luntz, A. C.; Keller, R. A.; Kim, H.; Gwinn, W. D. *J. Chem. Phys.* **1969**, *50*, 2438.
- (7) Pitzer, K. S.; Donath, W. E. *J. Am. Chem. Soc.* **1959**, *81*, 3213.
- (8) Ekejiuba, I. O. C.; Hallam, H. E. *Spectrochim. Acta* **1970**, *26A*, 59.
- (9) Ekejiuba, I. O. C.; Hallam, H. E. *Spectrochim. Acta* **1970**, *26A*, 67.
- (10) Wertz, D. W.; Shasky, W. E. *J. Chem. Phys.* **1971**, *55*, 2422.
- (11) Carreira, L. A. *J. Chem. Phys.* **1971**, *55*, 181.
- (12) Badawi, H. M.; Herrebout, W. A.; Zheng, C.; Mohamed, T. A.; van der Veken, B. J.; Durig, J. R. *Struct. Chem.* **2003**, *14*, 617.
- (13) Badawi, H. M.; Herrebout, W. A.; Mohamed, T. A.; van der Veken, B. J.; Sullivan, J. F.; Durig, D. T.; Zheng, C.; Kalasinsky, K. S.; Durig, J. R. *J. Mol. Struct.* **2003**, *645*, 89.
- (14) Guirgis, G. A.; El Defrawy, A. M.; Gounev, T. K.; Soliman, M. S.; Durig, J. R. *J. Mol. Struct.* **2007**, *832*, 73.
- (15) Guirgis, G. A.; El Defrawy, A. M.; Gounev, T. K.; Soliman, M. S.; Durig, J. R. *J. Mol. Struct.* **2007**, *834*, 17.
- (16) Möller, C.; Plesset, M. S. *Phys. Rev.* **1934**, *46*, 618.
- (17) Shellhamer, D. F.; Briggs, A. A.; Miller, B. M.; Prince, J. M.; Scott, D. H.; Heasley, V. L. *J. Chem. Soc., Perkin Trans. 2* **1996**, *2*, 973.
- (18) Durig, J. R.; Zheng, C.; Guirgis, G. A.; Wurrey, C. J. *J. Phys. Chem. A* **2005**, *109*, 1650.
- (19) Frisch, M. J.; Trucks, G. W.; Schlegel, H. B.; Scuseria, G. E.; Robb, M. A.; Cheeseman, J. R.; Montgomery Jr., J. A.; Vreven, T.; Kudin, K. N.; Burant, J. C.; Millam, J. M.; Iyengar, S. S.; Tomasi, J.; Barone, V.; Mennucci, B.; Cossi, M.; Scalmani, G.; Rega, N.; Petersson, G. A.; Nakatsuji, H.; Hada, M.; Ehara, M.; Toyota, K.; Fukuda, R.; Hasegawa, J.; Ishida, M.; Nakajima, T.; Honda, Y.; Kitao, O.; Nakai, H.; Klene, M.; Li, X.; Knox, J. E.; Hratchian, H. P.; Cross, J. B.; Adamo, C.; Jaramillo, J.; Gomperts, R.; Stratmann, R. E.; Yazyev, O.; Austin, A. J.; Cammi, R.; Pomelli, C.; Ochterski, J. W.; Ayala, P. Y.; Morokuma, K.; Voth, G. A.; Salvador, P.; Dannenberg, J. J.; Zakrzewski, V. G.; Dapprich, S.; Daniels, A. D.; Strain, M. C.; Farkas, O.; Malick, D. K.; Rabuck, A. D.; Raghavachari, K.; Foresman, J. B.; Ortiz, J. V.; Cui, Q.; Baboul, A. G.; Clifford, S.; Cioslowski, J.; Stefanov, B. B.; Liu, G.; Liashenko, A.; Piskorz, P.; Komaromi, I.; Martin, R. L.; Fox, D. J.; Keith, T.; Al-Laham, M. A.; Peng, C. Y.; Nanayakkara, A.; Challacombe, M.; Gill, P. M. W.; Johnson, B.; Chen, W.; Wong, M. W.; Gonzalez, C.; Pople, J. A. *Gaussian 03*, revision D.01; Gaussian, Inc.: Pittsburgh, PA, 2003.
- (20) Pulay, P. *Mol. Phys.* **1969**, *17*, 197.
- (21) Guirgis, G. A.; Zhu, X.; Yu, Z.; Durig, J. R. *J. Phys. Chem. A* **2000**, *104*, 4383.
- (22) Frisch, M. J.; Yamaguchi, Y.; Gaw, J. F.; Schaefer, H. F., III; Binkley, J. S. *J. Chem. Phys.* **1986**, *84*, 531.
- (23) Amos, R. D. *Chem. Phys. Lett.* **1986**, *124*, 376.
- (24) Polavarapu, P. L. *J. Phys. Chem.* **1990**, *94*, 8106.
- (25) Chantry, G. W. In *The Raman Effect*; Anderson, A., Ed.; Marcel Dekker Inc.: New York, 1971; Vol. 1, Chapter 2.
- (26) Lavrich, R. Private communication.
- (27) Durig, J. R.; Ng, K. W.; Zheng, C.; Shen, S. *Struct. Chem.* **2004**, *15*, 149.
- (28) Duncan, J. L.; Harvie, J. L.; McKean, D. C.; Cradock, S. *J. Mol. Struct.* **1986**, *145*, 225.
- (29) Villamanan, R. M.; Chen, W. D.; Wlodarczak, G.; Demaison, J.; Lesarri, A. G.; Lopez, J. C.; Alonso, J. L. *J. Mol. Spectrosc.* **1995**, *171*, 223.
- (30) Shen, Q.; Dakkouri, M. *J. Mol. Struct.* **1985**, *131*, 327.
- (31) Durig, J. R.; Zhao, W.; Zhu, X.; Geyer, T. J.; Dakkouri, M. *J. Mol. Struct.* **1995**, *351*, 31.
- (32) Hubbard, W. N.; Finke, H. L.; Scott, D. W.; McCullough, J. P.; Katz, C.; Gross, M. E.; Messerly, J. F.; Pennington, R. E.; Waddington, G. *J. Am. Chem. Soc.* **1952**, *74*, 6025.
- (33) Herschbach, D. R. *J. Chem. Phys.* **1956**, *25*, 358.
- (34) Durig, J. R.; Groner, P.; Griffin, M. G. *J. Chem. Phys.* **1977**, *66*, 3061.
- (35) Hirota, E.; Matsumura, C.; Morino, Y. *B. Chem. Soc. Jpn.* **1967**, *40*, 1124.
- (36) Trinkaus, A.; Dreizler, H.; Rudolph, H. D. *Z. Naturforsch. A* **1974**, *28*, 750.